Traceable Particle Swarm Optimization for Electromagnetically Navigated Bronchoscopy

Xiongbiao Luo[1], Takayuki Kitasaka[2], and Kensaku Mori[1,3]

[1] Information and Communications Headquarters, Nagoya University, Japan
[2] Faculty of Information Science, Aichi Institute of Technology, Japan
[3] Graduate School of Information Science, Nagoya University, Japan
xiongbiao.luo@gmail.com,
kitasaka@aitech.ac.jp,
kensaku@is.nagoya-u.ac.jp

Abstract. This paper proposes a modified evolutionary algorithm called traceable particle swarm optimization (PSO) that boosts bronchoscope motion tracking during electromagnetically navigated bronchoscopy. Since electromagnetic (EM) tracking is usually deteriorated by uncertainties (e.g., patient respiratory motion or magnetic field distortion) that occur in interventions, we develop a traceable PSO framework by integrating EM sensor measurements and image intensity information into the standard PSO method. In particular, all evolutionary parameters in our PSO framework can be updated traceably or adaptively in accordance with spatial distance constraints and image similarity information, resulting in an advantageous performance in dynamic bronchoscope motion estimation. Experimental results based on dynamic phantom validation demonstrate that our proposed tracking scheme provides a more robust, accurate, and efficient approach for endoscope motion tracking than several current available methods. The average tracking accuracy of position and orientation was improved from (4.3 mm, 7.8°) to (3.3 mm, 6.5°) and the computational time was reduced from 1.0 to 0.8 seconds per frame without any acceleration devices or code optimization strategy.

Keywords: Bronchoscope Motion Tracking, Electromagnetic Tracking, Particle Swarm Optimization, Electromagnetically Navigated Bronchoscopy.

1 Introduction

Endoscope location estimation or its motion tracking is the key component of any endoscope navigation systems, for instance, bronchoscope, colonscope, conchoscope, and neuroendoscope. Such a motion tracking procedure is usually formulated as an optimization process, which is commonly solved by deterministic [1–5, 9] or stochastic [6–8] approaches. Deterministic methods, typically intensity-based registration algorithms [3], usually define an optimization function to minimize the pixel difference between real video images and virtual bronchial renderings generated from pre-operative imaging information, for

C.A. Linte et al. (Eds.): AE-CAI 2012, LNCS 7815, pp. 105–116, 2013.

example, three-dimensional (3-D) data that are acquired by computed tomography (CT) or magnetic resonance imaging (MRI) scanners. Although image-based methods work well in bronchoscope motion tracking, they are somewhat constrained by bronchoscopic image artifacts (e.g., motion blurring) and easily get trapped in local minima during optimization. On the other hand, since EM trackers suffer from localization problems (e.g., patient airway deformation) and inaccurate EM sensor measurements (e.g., magnetic field distortion due to metallic materials in the working volume), stochastic methods, which take the randomness of bronchoscope movements into account, were introduced to deal with the dynamic uncertainties in bronchoscope motion tracking. Such methods seek the optimal of the posterior probability of one bronchoscope motion state, e.g., using sequential Monte Carlo (SMC) algorithms to generate a set of particles and propagate them to approximate the probability distribution of dynamic states. From experimental results [6–8], stochastic approaches were proved to be stable and accurate. Compared to deterministic methods, stochastic approaches show more robust and precise tracking performance but require more computational time to estimate six degrees of freedom (6DoF) motion parameters.

Even though many papers have been published on stochastic methods for improving electromagnetically navigated bronchoscopy [6–8], a more robust and accurate optimization approach is still greatly expected to tackle stochastic ambiguities in bronchoscope motion tracking. Recently, a numerous population-based stochastic evolutionary algorithm, particle swarm optimization (PSO), which was originally proposed by Kennedy and Eberhart [10], has been increasingly applied as a successful optimization technique to address multidimensional complex problems [12, 11, 13]. The algorithm simulates natural and biological behaviors such as birds flocking and fish schooling to find optimal solutions in nonlinear and high-dimensional spaces. Moreover, one of most attractive aspects of PSO is that it can tackle nonlinear, non-differentiable, and multi-modal optimization problems by dynamically interacting all particles in a similar analogy with the "cognitive" and "social" properties of populations [15, 14].

This work develops a traceable PSO framework for boosting EM tracking during electromagnetically navigated bronchoscopy. It is worthwhile to highlight the following aspects of our proposed approach. First, to the best of our knowledge, our proposed PSO framework is a novel application of PSO in endoscope motion tracking. We successfully formulated endoscope motion tracking as a PSO-based stochastic optimization process. Video image information and EM sensor measurements can be effectively integrated into PSO to achieve a robust and accurate tracking method, which also provides an effective means to fuse other external tracking sources in bronchoscopy navigation. Furthermore, using spatial constraints and image similarity, we modified PSO to automatically refresh evolutionary parameters for addressing the diversity loss problem, alleviating particle impoverishment, and obtaining various particle diversity in PSO iterations. Finally, our proposed approach combined ideas from evolutionary computation and medical image computing communities that should be applicable to other endoscopic guidances, e.g., conchoscope or colonscope.

This paper is generally organized as follows. We briefly review the basic PSO algorithm in Section 2. In Section 3, our proposed method for bronchoscope location or navigation is described in detail, by following our validation setups that are presented in Section 4. Experimental results are shown in 5 and discussed in 7 before concluding this work and giving future work in Section 7.

2 Particle Swarm Optimization

We here briefly review the standard PSO algorithm [10]. In PSO, a number of particles are utilized to denote the solutions in a dynamic system. Each particle i at iteration j and time k is represented by state vector $\mathbf{x}_k^{i,j} \in \Re^D$ associated with velocity vector $\mathbf{v}_k^{i,j} \in \Re^D$ that conducts particle transition and a corresponding fitness value that is determined by observation model $f(\mathbf{x}_k^{i,j})$. Given a particle set $\{\mathbf{x}_k^{i,j} \in \Re^D\}_{i=1}^N$ (N is the number of particles), in *j-th* iteration, particle state $\mathbf{x}_k^{i,j}$ and its velocity vector $\mathbf{v}_k^{i,j}$ are propagated to $\mathbf{x}_k^{i,j+1}$and $\mathbf{v}_k^{i,j+1}$ with inertia weight ω (to decide how much $\mathbf{v}_k^{i,j}$ to be preserved in $\mathbf{v}_k^{i,j+1}$) by:

$$\mathbf{v}_k^{i,j+1} = \omega \mathbf{v}_k^{i,j} + \lambda_1 \eta_1 (\mathbf{p}_k^{i,j} - \mathbf{x}_k^{i,j}) + \lambda_2 \eta_2 (\mathbf{g}_k^{i,j} - \mathbf{x}_k^{i,j}), \tag{1}$$

$$\mathbf{x}_k^{i,j+1} = \mathbf{x}_k^{i,j} + \mathbf{v}_k^{i,j+1}, \tag{2}$$

where λ_1 and λ_2 are acceleration constants and η_1 and η_2 are randomly generated from the uniform distribution with interval [0.0 1.0]. $\mathbf{p}_k^{i,j}$ (for the local individual best) and $\mathbf{g}_k^{i,j}$ (for the global all best) are the best state found by particle i so far and the best state found by the whole swarm so far, respectively.

After *j-th* iteration, $\mathbf{p}_k^{i,j}$ and $\mathbf{g}_k^{i,j}$ can be updated in accordance with each particle fitness value evaluated by $f(\mathbf{x}_k^{i,j+1})$:

$$\mathbf{p}_k^{i,j+1} = \begin{cases} \mathbf{x}_k^{i,j+1} & \text{if} f(\mathbf{x}_k^{i,j+1}) > f(\mathbf{p}_k^{i,j}) \\ \mathbf{p}_k^{i,j} & \text{otherwise} \end{cases}, \tag{3}$$

$$\mathbf{g}_k^{i,j+1} = \arg max_{\mathbf{p}_k^{i,j+1}} f(\mathbf{p}_k^{i,j+1}). \tag{4}$$

Based on Eqs. 1∼4, PSO tries to find the optimal solution during an optimization procedure. Please refer to [10] for more details about the basic PSO algorithm.

3 Proposed Tracking Framework

3.1 Overview

Our proposed framework to estimate bronchoscope motion consists of three main steps: (1) particle stochastic diffusion, (2) traceable analysis of evolutionary factors during particle propagation, and (3) the determination of bronchoscope motion parameters. During Step (1), a swarm of particles is generated and initialized. These particles are randomly propagated to increase the diversity.

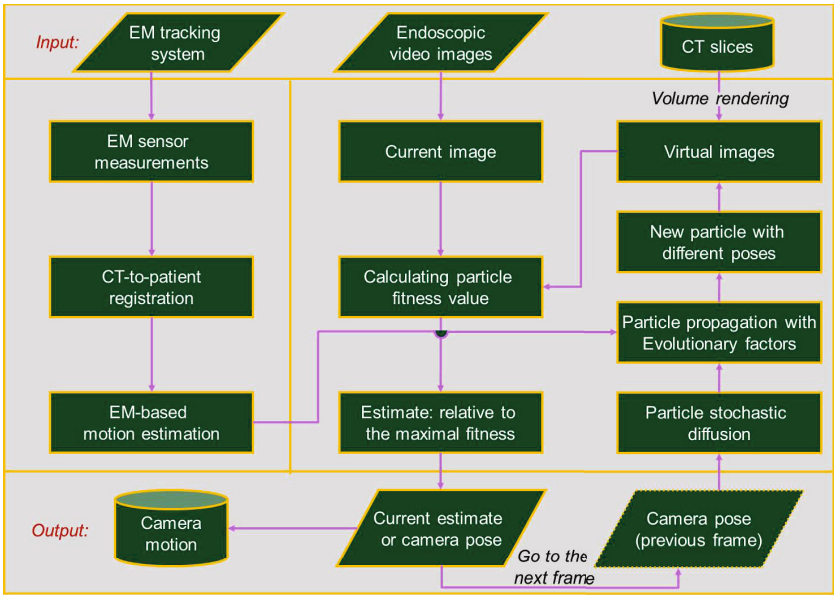

Fig. 1. The flowchart of bronchoscope 3-D motion estimation using our proposed method that comprises three steps of stochastic diffusion, particle propagation with adaptive evolutionary factors, and the determination of pose parameters

After that, evolutionary parameters including ω, λ_1, and λ_2 in Eqs. 1 and 2 are calculated in Step (2). Finally, PSO iterations are performed to determine the bronchoscope motion parameters or its pose information with position and orientation. Fig. 1 illustrates the proposed tracking framework to process CT slices, endoscopic video images, and EM sensor measurements for motion estimation.

3.2 Particle Stochastic Diffusion

We first define particle state $\mathbf{p}_k^{i,j}$ as a six-dimensional vector based on the bronchoscope position and orientation in our case of bronchoscope motion tracking:

$$\mathbf{p}_k^{i,j} = [t_x \quad t_y \quad t_z \quad \theta \quad \phi \quad \psi]^T, \tag{5}$$

where $\mathbf{p}_k^{i,j}$ corresponds to camera pose matrix $\mathbf{Q}_k(\mathbf{p}_k^{i,j}) = \mathcal{F}(t_x, t_y, t_z; \theta, \phi, \psi)$, translations t_x, t_y, and t_z and Euler angles θ, ϕ, and ψ of the bronchoscope camera around the x-, y-, and z-axes represent position and rotation, respectively.

Suppose that we generate a swarm of particles $\mathcal{P}_k^{i,j} = \{(\mathbf{p}_k^{i,j}, f(\mathbf{p}_k^{i,j}), \gamma_k^{i,j})\}_{i=1}^N$, where $\gamma_k^{i,j}$ is a weight based on spatial distance constraints. To increase the diversity of particles and avoid particle impoverishment, we perform a stochastic diffusion procedure in terms of the Gaussian propagation model and obtain $\mathbf{x}_k^{i,j}$:

$$\mathbf{x}_k^{i,j} = \mathcal{G}(\mathbf{p}_k^{i,j}, \mu \Delta \mathbf{s}_k), \tag{6}$$

where μ is a Gaussian distribution random number: $r \sim \mathcal{N}(0,1)$ and $\Delta\mathbf{s}_k$ is determined by EM-based motion estimates $\mathbf{s}_k$ and $\mathbf{s}_{k-1}$ at frames k and $(k-1)$:

$$\Delta\mathbf{s}_k = \mathbf{s}_k - \mathbf{s}_{k-1}, \mathbf{s}_k = [t_x^k\ t_y^k\ t_z^k\ \theta^k\ \phi^k\ \psi^k]_{EM}^T, \tag{7}$$

which is also used for initializing transition velocity $\mathbf{v}_k$: $\mathbf{v}_k = \Delta\mathbf{s}_k$ before it is updated by the global best solutions or estimates $\mathbf{g}_k$ and $\mathbf{g}_{k-1}$ during the iterations:

$$\mathbf{v}_k = \mathbf{g}_k - \mathbf{g}_{k-1}, \mathbf{g}_k = [t_x^k\ t_y^k\ t_z^k\ \theta^k\ \phi^k\ \psi^k]_{global}^T. \tag{8}$$

Note that our stochastic diffusion procedure for particle diversification does not perform a *resampling process*, as SMC or particle filter methods do [8], since the local best particles provide compact samples for propagation [13].

3.3 Parameter Traceable Analysis

Evolutionary parameters λ_1, λ_2, and ω heavily influence the PSO performance. Most current modified PSO algorithms do not consider spatial continuity constraint and image sequence information, which may result in a lack of systematic treatment of evolutionary states and expose PSO to a dangerous level of swarm explosion and divergence. To handle this limitation, we modify PSO based on image intensity to traceably control λ_1, and λ_2 by:

$$\lambda_1 = 2f(\mathbf{p}_k^{i,j})/f(\mathbf{p}_k^{i,j}) + f(\mathbf{g}_k^{i,j}), \quad \lambda_2 = 2f(\mathbf{g}_k^{i,j})/f(\mathbf{p}_k^{i,j}) + f(\mathbf{g}_k^{i,j}), \tag{9}$$

where $f(\mathbf{p}_k^{i,j})$ is defined as observation probability $Pr(\mathbf{o}_k^{i,j}|\mathbf{p}_k^{i,j})$:

$$f(\mathbf{p}_k^{i,j}) = Pr(\mathbf{o}_k^{i,j}|\mathbf{p}_k^{i,j}) = \delta_k^{i,j}(\sum_{i=1}^{N}\delta_k^{i,j})^{-1}, \tag{10}$$

where $\mathbf{o}_k^{i,j}$ is an observation corresponding to $\mathbf{p}_k^{i,j}$. $Pr(\mathbf{o}_k^{i,j}|\mathbf{p}_k^{i,j})$ depends on similarity $\delta_k^{i,j}$ between video image I_R^k and virtual rendering $I_V^k(\mathbf{Q}_k)$ generated at pose matrix $\mathbf{Q}_k(\mathbf{p}_k^{i,j})$ and $\delta_k^{i,j}$ is calculated based on image intensity by a modified mean square error ($MoMSE$) [8]:

$$\delta_k^{i,j} = MoMSE(I_R^k, I_V^k(\mathbf{p}_k^{i,j})). \tag{11}$$

For adaptively calculating ω, we utilize both fitness value $f(\mathbf{x}_k^{i,j}) \in [0\ 1]$ and particle spatial distribution information $\gamma_k^{i,j}$ among the particles. We first compute average distance $d_k^{i,j}$ from one particle to all other particles:

$$d_k^{i,j} = \frac{1}{N-1}\sum_{i=1, i\neq t}^{N}\sqrt{(\mathbf{x}_k^{i,j} - \mathbf{x}_k^{t,j})^2}. \tag{12}$$

After finding the largest distance d_{max} and the smallest distance d_{min} from $\{d_k^{i,j}\}_{i=1}^N$, we normalize distance $d_g^{i,j}$ between one particle and the current global best particle and obtain $\gamma_k^{i,j}$ and assign it to each particle:

$$\gamma_k^{i,j} = (d_g^{i,j} - d_{min})/(d_{max} - d_{min}), \quad \gamma_k^{i,j} \in [0\ 1]. \tag{13}$$

Finally, since ω was suggested within the interval [0.4 0.9] for weighting the global and the local searching abilities [14], we can traceably calculate it by:

$$\omega(f(\mathbf{x}_k^{i,j}), \gamma_k^{i,j}) = \frac{2}{2 + 3\exp(-1.28(f(\mathbf{x}_k^{i,j}) + \gamma_k^{i,j}))}, \tag{14}$$

which shows a novel strategy to automatically control ω in our modified PSO.

3.4 Bronchoscope Motion Estimation

Our work is to estimate to a full 6 degrees of freedom camera motion matrix $\mathbf{Q}_k$ including camera position and orientation. We integrate EM sensor measurements and image similarity information into our modified PSO algorithm discussed above. The output of the POS tracking framework is represented by:

$$\mathbf{Q}_k^*(g_k^*) = \mathcal{F}(t_x^g, t_y^g, t_z^g; \theta^g, \phi^g, \psi^g) = \begin{pmatrix} \mathbf{R}_k & \mathbf{t}_k \\ \mathbf{0}^T & 1 \end{pmatrix}, \tag{15}$$

where $\mathbf{t}_k = [t_x^g, t_y^g, t_z^g]^T$ and rotation matrix $\mathbf{R}_k$ are related to θ^g, ϕ^g, and ψ^g:

$$\mathbf{R}_k = \begin{pmatrix} C_3C_2 & C_3S_2S_1 - S_3C_1 & C_3S_2C_1 + S_3S_1 \\ S_3C_2 & S_3S_2S_1 + C_3C_1 & S_3S_2C_1 - C_3S_1 \\ -S_2 & C_2S_1 & C_2C_1 \end{pmatrix}, \tag{16}$$

where $S_1 = \sin\theta^g$, $S_2 = \sin\phi^g$, $S_3 = \sin\psi^g$, $C_1 = \cos\theta^g$, $C_2 = \cos\phi^g$, and $C_3 = \cos\psi^g$. The implementation of our proposed method for improving EM tracking and boosting navigated bronchoscopy is summarized in Algorithm 1.

Algorithm 1. Traceable PSO for Bronchoscope Motion Estimation

input : Bronchoscopic video images $\mathbf{I}_R^k$, CT-based virtual images $\mathbf{I}_V$, and electromagnetic sensor measurements $\mathbf{s}_k$
output: All global best estimates $\mathbf{Q}_k^*(g_k^*)$ of bronchoscope camera poses

1. Initialization: At time $k = 0$, use $\mathbf{Q}_0$ to initialize $\mathcal{P}_0^{i,j}$ and $\mathbf{g}_0^{i,j}$;
2. Perform stochastic diffusion to obtain $\{\mathbf{x}_0^{i,j}\}$ by Eq. 6;
3. Compute $f(\mathbf{p}_0^{i,j})$ by Eq. 10 and update $\mathcal{P}_0^{i,j}$ and $\mathbf{g}_0^{i,j}$ by Eqs. 3 and 4;
4. Implement Traceable PSO iterations:

```
for k = 1 to T (frame number) do
    for j = 1 to M (iteration number) do
        Update evolutionary parameters ω, λ1, and λ2 by Eqs. 9 and 14;
        for i = 1 to N (particle number) do
            Perform PSO iteration in accordance with Eqs. 1 and 2;
            Update each particle x_k^{i,j} and velocity vector v_k^{i,j};
            Compute f(p_k^{i,j}) and γ_k^{i,j} by Eqs. 10 and 13;
        end
        Update particle set P_k^{i,j} and global best particle g_k^{i,j} by Eqs. 3 and 4;
    end
    Find global best estimate g_k^* from particle set P_k^{i,j};
    Determine motion pose: Q_k^*(g_k^*) ⟺ F(t_x^g, t_y^g, t_z^g; θ^g, φ^g, ψ^g) by Eq. 15;
end
```

5. Return: all $\{\mathbf{Q}_k^*(g_k^*)\}_{k=1}^T$

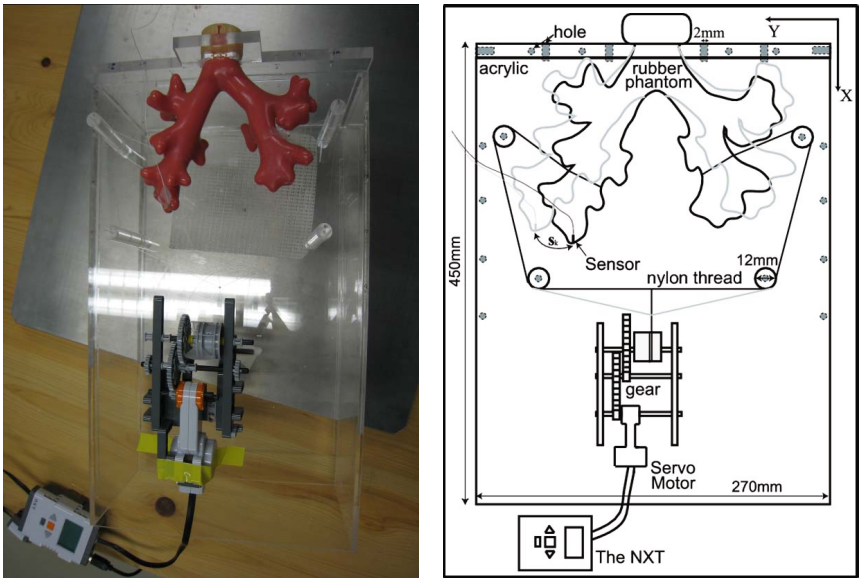

(a) (b)

Fig. 2. The dynamic phantom was constructed with the airway tree rubber, a motor, and nylon thread. (a) physical phantom and (b) phantom movement.

Fig. 3. The EM tracking system that was used here includes the control unit (*left*) and the fat-type magnetic field generator (*right*)

4 Experimental Setups

4.1 Hardwares

We evaluated our proposed tracking method on a dynamic phantom with an adjustable motion: $0 \sim 24$ mm, as shown in Fig 2. The CT spacing parameters of our phantom were: 512×512 pixels, 1021 slices, 0.68-mm reconstruction pitch, and 0.5-mm thick slices. A 3-D Guidance medSAFE tracker (Ascension Technology Corporation, USA) was used as an EM tracking system, which includes a 9-coil at flat-type transmitter as a magnetic field generator, as illustrated in Fig. 3. Endoscopic video images of size 362×370 pixels were recorded at 30 frames per second using an endoscope (BF-P260F, Olympus, Tokyo).

4.2 Ground Truth

To evaluate the tracking accuracy of different methods, we generated five ground truth datasets (GTDs) by manually adjusting the position and orientation of the virtual camera to qualitatively register the real and virtual bronchoscopic viewing points by hand. Three observers of the authors independently and repeatedly collected these GTDs in multiple sessions. We clarify that intra-observer consistency was 1.81 mm and 5.9°, 1.76 mm and 4.9°, and 1.93 mm and 4.8° from three observers, respectively; inter-observer consistency was 1.71 mm and 5.6°. Note that the clinical requirement of position and orientation is below 2 mm and 6° during bronchoscopic interventions.

We compared five tracking approaches (1) M1: only using EMT tracking reported by Schwarz et al. [16], (2) M2: a hybrid method presented by Mori et al. [4], (3) M3: a modified hybrid method proposed by Luo et al. [17], (4) M4: a SMC-based solution introudced by Luo et al. [8], and (5) our proposed framework, as discussed in Section 3. Additionally, we set the particle number: $N = 50$ and the iteration number: $M = 10$. During the SMC-based tracking, the particle number was set to 500. We have done all implementations on a Microsoft Visual C++ platform and ran it on a conventional PC (CPU: Intel(R) Xeon(R) X5482 $\times 2$ processors, 16-GByte main memory).

5 Results

Table 1 displays the quantitative results of the tracking accuracy from different methods. The average position and orientation errors of the proposed framework were 3.3 mm and 6.5°, which are definitely better than those of the previous published methods that had average errors of at least 4.3 mm and 7.8°. We also visually inspected the tracking results by manually checking whether the real images resembled the virtual images. Fig. 4 shows examples of real images and the corresponding virtual images generated from the camera parameters

Table 1. Quantitative results of tracking accuracy of compared methods in terms of position and orientation errors between estimated results and ground truth

Experiments	Data 1	Data 2	Data 3	Data 4	Data 5
Max Motion	2.5 mm	5.6 mm	10.4 mm	13.8 mm	22.3 mm
M1 [16]	4.2±2.6 mm 6.7±5.2°	5.3±3.5 mm 8.8±6.2°	5.6±2.8 mm 7.9±5.3°	6.0±2.6 mm 9.6±6.0°	7.2±3.5 mm 13.5±11.1°
M2 [4]	3.8±3.2 mm 6.1±4.1°	4.9±4.2 mm 7.6±5.5°	5.4±3.2 mm 6.8±6.2°	5.8±3.6 mm 8.8±5.6°	6.8±4.4 mm 12.9±13.4°
M3 [17]	3.4±2.6 mm 5.3±3.2°	4.6±3.5 mm 6.7±2.9°	5.3±4.1 mm 5.6±5.2°	5.6±4.8 mm 10.6±5.8°	6.1±4.6 mm 12.7±11.8°
M4 [8]	3.1±2.2 mm 4.8±4.2°	3.9±2.1 mm 5.8±3.2°	4.1±2.5 mm 6.2±3.1°	4.6±3.2 mm 9.5±5.5°	5.6±4.3 mm 12.9±12.6°
Our method	2.6±2.4 mm 3.9±2.2°	2.9±1.9 mm 4.2±2.6°	3.2±2.6 mm 5.2±3.6°	3.5±2.9 mm 8.9±5.2°	4.4±3.0 mm 10.2±10.5°

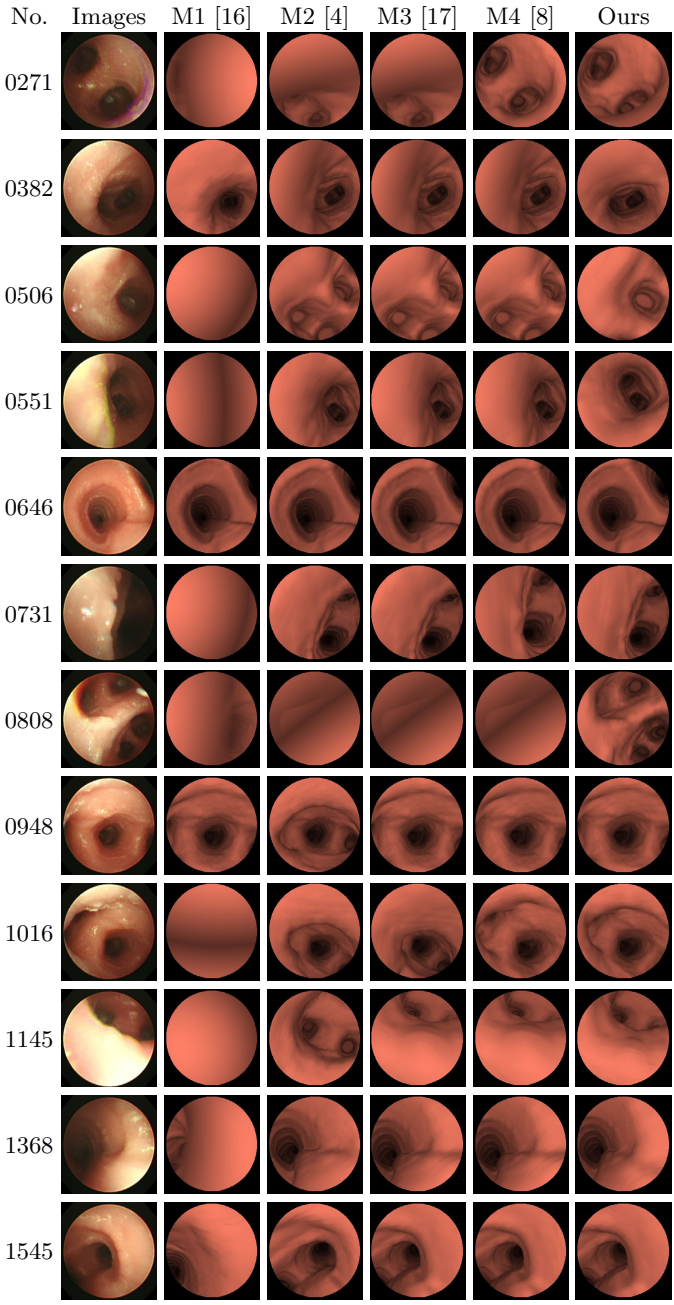

Fig. 4. Visual comparison of tracking results of Data 4. Left column shows selected frame numbers, and second column gives their corresponding video images. Other columns display virtual bronchoscopic images generated from tracking results using methods discussed above. Our method shows the best performance.

estimated by each method. This visual investigation of the successfully processed frames further demonstrates the effectiveness of our proposed method. Additionally, the current runtime of our method is about 0.8 seconds per frame, which outperforms that reported in [5] by speed-up devices (0.98 seconds).

6 Discussion

Generally, our proposed PSO tracking method provides a more accurate and robust strategy to estimate endoscope motion than previous approaches. We attribute such an advantageous performance of our PSO framework tracking to the following aspects. First, we believe that our traceable PSO is partly an association of PSO iterations and SMC sampling procedures, and hence it outperforms the SMC sampling algorithms in motion tracking. During SMC sampling procedures, a successful particle sampling depends heavily on the proposal distribution function [18]. Particles with large weights located in the useful area of the proposal distribution are usually sampled. In fact, the proposal distribution is suggested to be the dynamic transition distribution, which may incur particles with larger weight that are not sampled when the useful area of the transition distribution stays at the tail of the observation distribution [18]. However, the PSO framework performs more like a hierarchical sampling strategy which propagates the particles integrated with the newest observations [11], possibly resolving the particle impoverishment problem. Next, automatically or traceably controlling evolutionary parameters is greatly helpful to update particles in iterations. The two acceleration factors, which were calculated based on the fitness value from the image intensity information, are more reasonable than setting them to 2 in standard PSOs [10]. Moreover, the inertia weight is also adaptively determined by both spatial distance constraint and image intensity information, resulting in more flexibly balancing the global and local search abilities and providing a reasonable velocity limitation to move particles. Finally, without any *resampling process* in our method, compared to SMC sampling or particle filtering, it is helpful to reduce the runtime of our method.

Additionally, we must clarify the potential limitations of our proposed methods. Particle robustness, which means the particle fitness value to be correctly computed and evaluate, depends somewhat on image intensity information. However, the image artifacts that occur in bronchoscopic video may collapse the correct computation of the fitness value. To tackle this drawback, a more robust intensity similarity measure, which should be slightly insensitive to illumination changes or other image artifacts, must be developed in future work. Another problem remains how to properly choose the particle and iteration numbers M and N. In fact, it is difficult to know their influences on the tracking performance. Thoroughly evaluating M and N in PSO is another future work. We plan to adaptively select them by particle robustness during iterations, possibly reducing our current runtime, which is also future work.

7 Conclusions

This work proposes a new bronchoscope 3-D motion tracking framework for endoscope location or navigation using a traceable PSO algorithm that can refresh its evolutionary parameters based on spatial distance constraints and image intensity information during iterations. Dynamic phantom validation proves that our method provides a more advantageous tracking performance than state-of-the-art methods. Future work also includes reducing the runtime of our method.

Acknowledgment. This work was partly supported by the Center of Excellence project "Development of Bedside Medical Devices for High Precision Diagnosis of Cancer in Its Preliminary Stage" (01-D-D0806) funded by the Aichi Prefecture, and "Computational anatomy for computer-aided diagnosis and therapy: frontiers of medical image sciences" (21103006) funded by the Grant-in-Aid for Scientific Research on Innovative Areas, MEXT, Japan.

References

1. Deligianni, F., Chung, A.J., Yang, G.Z.: Nonrigid 2-D/3-D registration for patient specific bronchoscopy simulation with statistical shape modeling: Phantom validation. IEEE TMI 25(11), 1462–1471 (2006)
2. Helferty, J.P., Sherbondy, A.J., Kiraly, A.P., Higgins, W.E.: Computer-based system for the virtual-endoscopic guidance of bronchoscopy. CVIU 108(1-2), 171–187 (2007)
3. Deguchi, D., Mori, K., Feuerstein, M., Kitasaka, T., Maurer Jr., C.R., Suenaga, Y., Takabatake, H., Mori, M., Natori, H.: Selective image similarity measure for bronchoscope tracking based on image registration. MedIA 13(4), 621–633 (2009)
4. Mori, K., Deguchi, D., Akiyama, K., Kitasaka, T., Maurer Jr., C.R., Suenaga, Y., Takabatake, H., Mori, M., Natori, H.: Hybrid bronchoscope tracking using a magnetic tracking sensor and image registration. In: Duncan, J.S., Gerig, G. (eds.) MICCAI 2005, Part II. LNCS, vol. 3750, pp. 543–550. Springer, Heidelberg (2005)
5. Reichl, T., Luo, X., Menzel, M., Hautmann, H., Mori, K., Navab, N.: Deformable registration of bronchoscopic video sequences to CT volumes with guaranteed smooth output. In: Fichtinger, G., Martel, A., Peters, T. (eds.) MICCAI 2011, Part I. LNCS, vol. 6891, pp. 17–24. Springer, Heidelberg (2011)
6. Gergel, I., dos Santos, T.R., Tetzlaff, R., Maier-Hein, L., Meinzer, H.-P., Wegner, I.: Particle filtering for respiratory motion compensation during navigated bronchoscopy. In: Wong, K.H., Miga, M.I. (eds.) SPIE Medical Imaging 2010, California, USA, vol. 7625, p. 76250W (2010)
7. Soper, T.D., Haynor, D.R., Glenny, R.W., Seibel, E.J.: In vivo validation of a hybrid tracking system for navigation of an ultrathin bronchoscope within peripheral airways. IEEE TBME 57(3), 736–745 (2010)
8. Luó, X., Reichl, T., Feuerstein, M., Kitasaka, T., Mori, K.: Modified hybrid bronchoscope tracking based on sequential monte carlo sampler: Dynamic phantom validation. In: Kimmel, R., Klette, R., Sugimoto, A. (eds.) ACCV 2010, Part III. LNCS, vol. 6494, pp. 409–421. Springer, Heidelberg (2011)

9. Luo, X., Kitasaka, T., Mori, K.: Bronchoscopy navigation beyond electromagnetic tracking systems: A novel bronchoscope tracking prototype. In: Fichtinger, G., Martel, A., Peters, T. (eds.) MICCAI 2011, Part I. LNCS, vol. 6891, pp. 194–202. Springer, Heidelberg (2011)
10. Kennedy, J., Eberhart, R.C.: Particle swarm optimization. In: Proc. IEEE International Conf. on Neural Networks, pp. 1942–1948 (1995)
11. Zhang, X., Hu, W., Qu, W., Maybank, S.: Multiple object tracking via species-based particle swarm optimization. IEEE TCSVT 20(11), 1590–1602 (2010)
12. John, V., Trucco, E., Ivekovic, S.: Markerless human articulated tracking using hierarchical particle swarm optimisation. IVC 28(11), 1530–1547 (2010)
13. Zhang, L., Mei, T., Liu, Y., Tao, D., Zhou, H.-Q.: Visual search reranking via adaptive particle swarm optimization. Pattern Recognition 44(8), 1811–1820 (2011)
14. Parrott, D., Li, X.: Locating and tracking multiple dynamic optima by a particle swarm model using speciation. IEEE TEC 10(4), 440–458 (2006)
15. Clerc, M., Kennedy, J.: The particle swarm-explosion, stability and convergence in a multidimensional complex space. IEEE TEC 6(1), 58–73 (2002)
16. Schwarz, Y., Greif, J., Becker, H.D., Ernst, A., Mehta, A.: Real-time electromagnetic navigation bronchoscopy to peripheral lung lesions using overlaid CT images: the first human study. Chest 129(4), 988–994 (2006)
17. Luo, X., Feuerstein, M., Imaizumi, K., Hasegawa, Y., Mori, K.: Towards hybrid bronchoscope tracking under respiratory motion: evaluation on a dynamic motion phantom. In: Wong, K.H., Miga, M.I. (eds.) SPIE Medical Imaging 2010, California USA, vol. 7625, p. 76250B (2010)
18. Arulampalam, M., Maskell, S., Gordon, N., Clapp, T.: A tutorial on particle filters for nonlinear/non-gaussian Bayesian tracking. IEEE TSP 50(2), 174–188 (2002)